# NON-FERMI-LIQUID PROPERTIES AND EXOTIC SUPERCONDUCTIVITY IN $CeCu_2Si_2$ AND $(\underline{U}Th)Be_{13}$

M. Lang[1], P. Gegenwart[1], R. Helfrich[1], M. Köppen[2], F. Kromer[1], C. Langhammer[1], C. Geibel[1], F. Steglich[1,2], J.S. Kim[3], G.R. Stewart[3,4]

[1]Max-Planck-Institut für Chemische Physik fester Stoffe, D-01187 Dresden Germany
[2]Institut für Festkörperphysik, SFB 252, TU Darmstadt, D-64289 Darmstadt Germany
[3]Department of Physics, University of Florida, Gainesville, Florida 32611, USA
[4]Institut für Physik, Universität Augsburg, D-86159 Augsburg, Germany

## INTRODUCTION

Tetragonal $CeCu_2Si_2$ [1] and cubic $UBe_{13}$ [2] belong to the class of strongly correlated f-electron materials where a periodic lattice of partially filled f shells is embedded in a metallic environment. Below a characteristic "Kondo temperature" $T_K$, typically of the order of 10K, quasiparticles composed of both local f degrees of freedom and itinerant conduction-electron degrees of freedom form. As has been inferred from the giant Sommerfeld coefficient $\gamma$ of about 1 $J/K^2$mole, the huge effective quasiparticle masses $m^*$ (100 - 1000 $m_{el}$) are governed by the f degrees of freedom. The discontinuity of the specific heat at $T_c$ which was found to scale with the large $\gamma$ [1,2] proved that superconductivity is, indeed, formed by those heavy fermions (HF).

In the years that followed the discovery of HF superconductivity, the number of systems showing similar properties has grown. Compared to their later discovered counterparts $UPt_3$ [3], $URu_2Si_2$ [4], $UNi_2Al_3$ [5] and $UPd_2Al_3$ [6], it appears that $CeCu_2Si_2$ and $UBe_{13}$ reveal a more complex phenomenology and are less understood. For $CeCu_2Si_2$, an as yet unidentified, presumably magnetically ordered "phase A" has been found which is almost degenerate with HF superconductivity. Further on, the low-temperature normal state is characterized by strong violations of the behavior expected for a Landau Fermi liquid. This holds true also for the normal-conducting state of $UBe_{13}$. For the latter, particular interest arose, however, because of its highly anomalous superconducting-state properties, notably the occurrence of a double phase transition for weakly Th doped $U_{1-x}Th_xBe_{13}$ [7].

In this paper we summarize our recent works [8-10] on these two canonical HF superconductors. Two main aspects will be addressed: In Sects. 2 and 3 we will explore their

non-Fermi-liquid properties. We will investigate whether this behavior is related to the nearness of a quantum critical point, defined by a magnetic ordering temperature $T_m \to 0$. If so, we will study how heavy fermions behave in its vicinity. In Sect. 4 we will address our recent discovery of a "new line of anomalies" in the superconducting state of $UBe_{13}$ and its thoriated variant $U_{1-x}Th_xBe_{13}$. Our results call for a revision of the interpretation of the low-T phases in the complex T-x phase diagram that had been established for this system.

## 2. $CeCu_2Si_2$

### 2.1 Different ground-state behaviors

By means of a thorough thermodynamic investigation of $CeCu_2Si_2$ single crystals it was found that distinctly different ground-state properties exist which depend sensitively on the composition of the starting melt and/or the subsequent heat treatment [11,12]. This can be most clearly visualized by comparing the coefficient of thermal expansion, $\alpha(T) = l^{-1}dl/dT$, for such differently prepared single crystals (Fig. 1). The transition from the paramagnetic into the superconducting state manifests itself in a positive jump in $\alpha$ measured along the a-axis [11]. This is shown in Fig. 1a for an annealed single crystal with $T_c = 0.63$K. In an overcritical field of B = 3 T superconductivity is suppressed and no indication for any further anomaly can be resolved in $\alpha(T)$ down to 0.05 K. For a number of unannealed crystals it was found, however, that instead of bulk superconductivity they showed a transition into phase A with an onset temperature $T_A \approx 0.7$ K. This is accompanied by a large negative discontinuity in $\alpha(T)$, cf. Fig.1b. Measurements in B = 3 T demonstrate that compared to superconductivity, phase A is much more robust against magnetic fields. For other crystals, an intermediate behavior was found [12] (Fig. 1c): Upon cooling an incipient A-phase transition is replaced by the superconducting transition at $T_c \approx 0.67$ K. In an overcritical field of B = 1.5 T, superconductivity is suppressed and phase A fully recovers. These astonishing differences in the ground-state properties of $CeCu_2Si_2$ are most likely related to variaticns in site occupation within the single crystals. However, no significant difference in the lattice constants could be resolved by X-ray diffractometry. Using polycrystalline $Ce_{1+x}Cu_{2+y}Si_{2+z}$ samples with compositions deliberately chosen to be slightly off stoichiometric it was possible to map those different ground-state behaviors onto separate sectors of the narrow homogeneity range of the primary $CeCu_2Si_2$ phase within the ternary Ce-Cu-Si phase diagram [13]. While samples prepared with slight Cu excess show superconductivity without phase A, a transition into phase A is found in those samples with Cu/Ce deficiency. Both the "S" and "A" sectors are separated from each other by the "AS" sector containing the true stoichiometric point. The thermal expansion of a polycrystalline sample out of the "AS" sector is displayed in Fig.1d.

### 2.2 On the nature of phase A

The nature of phase A is still unknown. Neutron diffractometry has so far failed to resolve magnetic Bragg reflections. Different assignments spanning the whole range from spin-glass [14] to dynamical [15] and unconventional spin-density-wave [16] order have been made. Partial Ge substitution for Si was found to stabilize phase A and to support strong evidence for an antiferromagnetic transition at $T_A$ [17]. For all $CeCu_2Si_2$ samples studied so far, an additional "phase B" [12] phenomenologically related to phase A, was found to form at fields B > 6T. Below we focuss on single crystals of the "AS" sector where phase A can be studied when

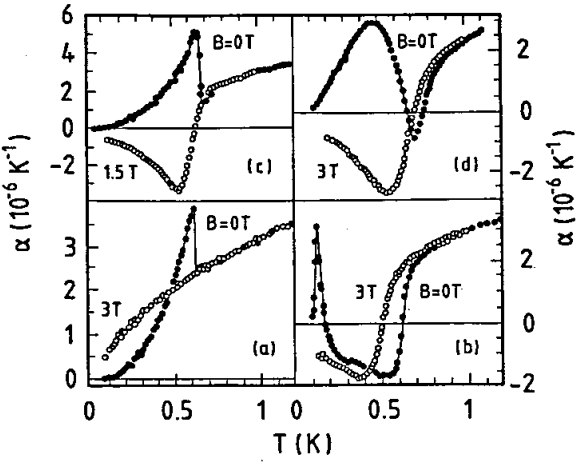


Fig.1. Coefficient of thermal-expansion measured parallel to the a axis as a function of temperature at both B = 0 and B > $B_{c2}(0)$, with B∥a, for three $CeCu_2Si_2$ single crystals: a) superconducting crystal identical to that studied in [11]; b) non-bulk-superconducting crystal ("as grown") [11]. c) same crystal as studied in [12] showing a superconducting transition in B = 0 but a transition into "phase A" at B > $B_{c2}$; In d) one third of the volume-expansion coefficient, $\alpha(T) = 1/3 \cdot \beta(T)$, at B = 0 T and 3 T is shown for a polycrystalline sample from the same type as the single crystal in c).

superconductivity has been suppressed by a sufficiently large magnetic field. Fig. 2 shows the normalized resistivity measured along the respective a- and c-axes in an overcritical field B = 5T. The additional scattering contribution visible at low temperatures marks the transition from the paramagnetic phase into phase A. As will be discussed in Sect 2.3 in more detail, phase A (and B) develops out of a state where the resistivity varies as $\rho(T) = \rho_0 + aT^2$ ($\rho_0$: residual resistivity) with a giant coefficient $a \approx 10\ \mu\Omega cmK^{-2}$. The resistivity contribution $\delta\rho = \rho(T) - (\rho_0 + aT^2)$ associated with the transition at $T_A$ is shown in the insert. While $\delta\rho$ increases below $T_A$ for current j∥a, no change is found in $\delta\rho$ for j∥c at this temperature. This is consistent with a

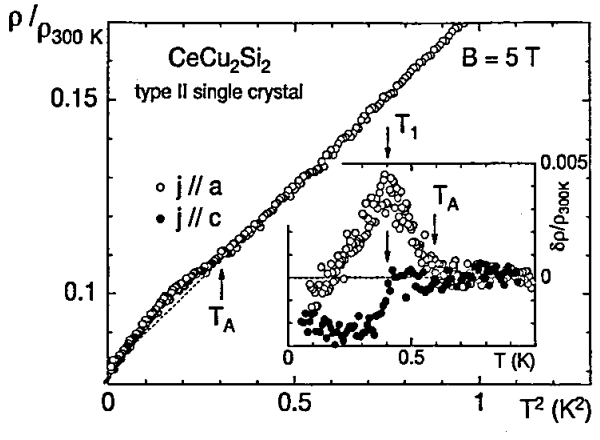


Fig. 2. Normalized resistivity versus $T^2$ for the "AS-type" $CeCu_2Si_2$ single crystal at a field B = 5 T for current j∥a (B∥c). Inset shows $\delta\rho = \rho - \rho_0 - aT^2$, measured along the respective a- and c- axes at the same field (applied perpendicular to the current).

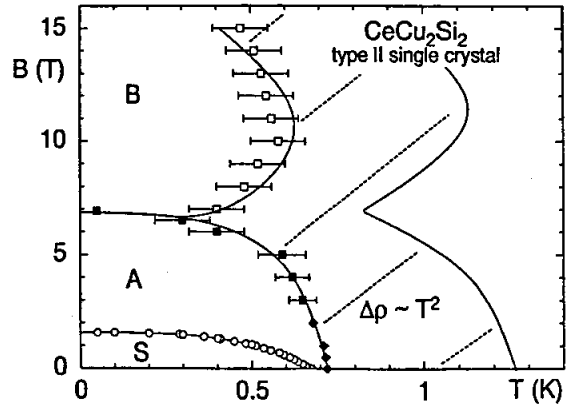


Fig.3. B-T diagram, based upon resistivity results, for the "AS-type" $CeCu_2Si_2$ single crystal. Validity range for the $T^2$-law is indicated.

transition into a SDW state with a nesting vector lying within the basal plane, see, e.g. [18]: The increase in $\delta\rho$ for $j \| a$ reflects the reduction of the effective carrier number, while the isotropic decrease at somewhat lower temperatures may indicate the freezing out of incoherent scattering. The resistively determined B-T phase diagram is shown in Fig. 3 which also includes the high-field phase B as well as the validity range of the $\rho \propto T^2$ behavior.

In order to study the phase boundary between the A and B phase in great detail, we have performed low-temperature magnetostriction measurements. Fig. 4 shows relative length changes, $\Delta l/l$, as a function of field at T = 0.25 K. From the discontinuous behavior of $\Delta l/l$ at 6.8T - the A-B phase boundary - the first-order character of this transition can be inferred. Similar observations [19] have been made on the "AS" crystal studied in [12]. These observations are consistent with a field-induced transition between different SDW states as has been established for the quasi-onedimensional organic salts [20]. In addition, Fig. 4 provides

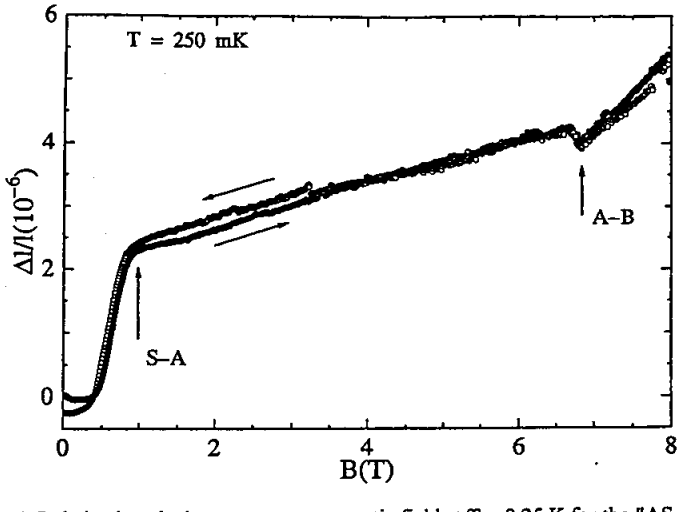


Fig. 4. Relative length changes versus magnetic field at T = 0.25 K for the "AS-type" $CeCu_2Si_2$ single crystal. Arrows indicate the respective phase transitions between the superconducting (S) and A phase (S-A) as well as A and B phase (A-B).

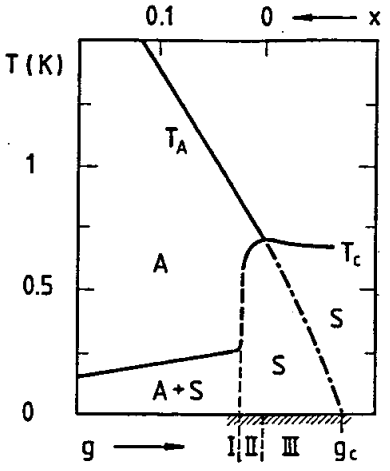


Fig. 5. Schematic phase diagram for $CeCu_2Si_2$ at zero field, indicating existence ranges for phase A (A), superconductivity (S) and coexistence range (A+S). For samples labeled "type I" ("A" type), "II" ("AS" type) and "III" ("S" type): $T_A > T_c$, $T_A \geq T_c$ and $T_A < T_c$, respectively (see text). On the abscissa an effective coupling constant g is used. The phase boundaries $T_A(g)$ [17,23] and $T_c(g)$ [22,23] are determined from B = 0 measurements (solid lines) or extrapolated from data taken at $B > B_{c2}$ [22,23] (dash-dotted line).

evidence that as a function of field the transition from the superconducting state at small fields to the A phase at intermediate fields is of first order, too. This reflects the field-induced

Taken together, our results indicate that $T_A$ marks the transition into a SDW state with a nesting vector lying within the basal plane.

### 2.3 Break-up of heavy fermions on the brink of "phase A"

As mentioned before, phase A can be stabilized by partial Ge-substitution for Si [17]. Polycrystalline $CeCu_2(Si_{1-x}Ge_x)_2$ samples with $0.02 < x < 0.15$ and undoped samples of type A exhibit an A-phase transition between $T_A \approx 0.8$ K and 1.75 K, followed by a bulk HF-superconducting transition between $T_c \approx 0.3$ K and 0.15 K, respectively, cf. the phase diagram in Fig. 5. Phase A and (thermodynamically weak) superconductivity coexist on a microscopic scale [21]. In "AS" type $CeCu_2Si_2$ samples of near stoichiometric composition and with $T_A \geq T_c$, (thermodynamically strong) HF superconductivity expells phase A [12]. Bulk measurements of "S"-type $CeCu_2Si_2$ polycrystals reveal A-phase signatures only at magnetic fields sufficient to suppress superconductivity. From the B-T phase diagrams collected for such polycrystals yielding fictitious transition temperatures $T_A(B=0) \approx 0.5$ K and 0.35 K [22] we infer that via suitable composition the A phase can be tuned to $T_A \to 0$. In the phase diagram in Fig. 5, an effective coupling constant g measuring the strength of the 4f hybridization with the conduction electrons is used on the abscissa. g is expected to be a complicated function of the composition in homogeneous $CeCu_2Si_2$ samples [24] and to be proportional to the Ge-content, x, in $CeCu_2(Si_{1-x}Ge_x)_2$. Fig. 5 suggests the existence of a critical coupling constant $g_c$ at which $T_A \to 0$. From the absence of any A-phase signatures for our single crystals of type "S" a coupling constant slightly in excess of $g_c$ can be expected. In the following, we will discuss, whether $g_c$ defines a quantum critical point (QCP) and, if so, how heavy fermions behave in its vicinity.

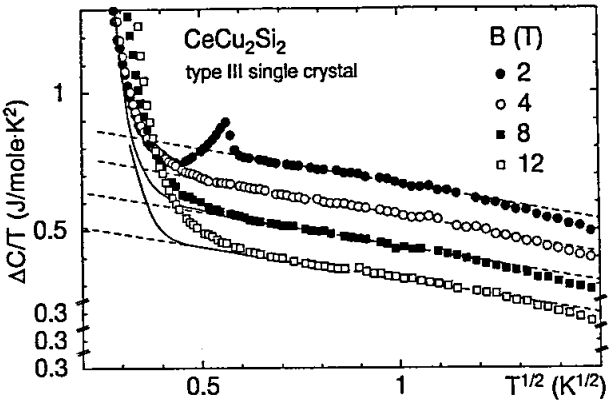


Fig.6. Ce-increment to the specific heat as $\gamma = \Delta C/T$ vs $T^{1/2}$ at varying fields for the "AS-type" $CeCu_2Si_2$ single crystal. Dashed lines indicate $(-T^{1/2})$ dependence of $\gamma(T) - \gamma_0$. Solid lines display $\Delta C(T)/T$ data after subtraction of nuclear hyperfine contributions due to the applied fields. For B = 2 T, the superconducting transition anomaly at $T_c \approx 0.3$ K is seen.

It has been predicted that close to an antiferromagnetic (AF) QCP, low-lying and spatially extended spinfluctuations with wave vector $\mathbf{q} \approx \mathbf{Q}$, the afm ordering wavevector, give rise to strongly T-dependent quasiparticle masses and quasiparticle-quasiparticle cross sections [25-27]. For threedimensional (3D) systems these should manifest themselves in coefficients $\gamma = C/T$ and $a = (\rho - \rho_0)/T^2$ in the specific heat and resistivity which are not constant as in a Landau Fermi liquid, but obey the following asymptotic T dependences [26,27]:

$$\gamma(T) = \gamma_0 - \alpha T^{1/2} \quad (1)$$

and [25-27]

$$a(T) = \beta T^{-1/2} \quad (2a)$$

corresponding to

$$\Delta\rho = \rho(T) - \rho_0 = \beta T^{3/2} \quad (2b).$$

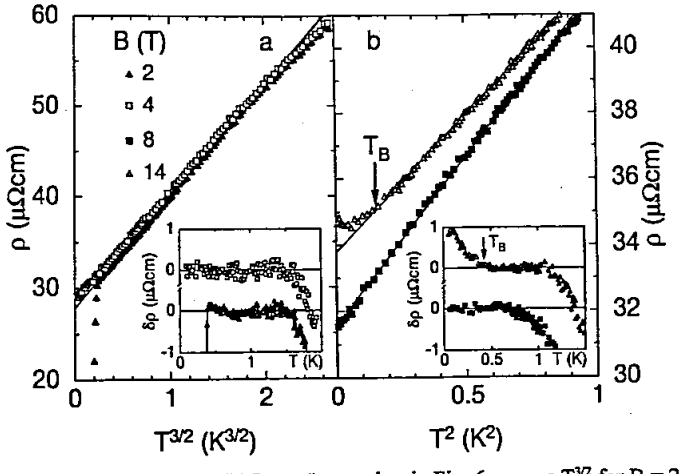


Fig.7. Resistivity for the same "AS-type" crystal as in Fig. 6 as $\rho$ vs $T^{3/2}$ for B = 2 T and 4 T (a) as well as $\rho$ vs $T^2$ for B = 8 T and 14 T (b). Insets show $\delta\rho$ vs T with $\delta\rho = \rho - \rho_0 - \beta T^{3/2}$ (a) and $\delta\rho = \rho - \rho_0 - \beta T^2$ (b), respectively. Arrows in (b) indicate B-phase transition for B = 14 T.

Since the singular scattering expressed by Eq. 2a is associated with the AF wavevector **Q**, i.e. occurs only along certain "hot lines" on the Fermi surface, all other quasiparticle-quasiparticle scattering events ought to give rise to the ordinary Fermi liquid term $\Delta\rho \propto T^2$ (a=const) which, consequently, must short-circuit the anomalous $\beta T^{3/2}$ term at sufficiently low temperatures [28]. In Figs. 6 and 7 we show results of $\gamma(T)$ and $\Delta\rho(T)$ for an "S"-type single crystal which lacks any A-phase signature. Let us first focus on the data taken at sufficiently low fields ($B < 6T$) and intermediate temperatures, cf. Figs. 6 and 7a. For $T > 0.2$ K and $B < 6$ T, both $\gamma(T)$ and $\Delta\rho(T)$ obey Eqs. 1 and 2b for $T < 1.7$ K suggesting the existence of an AF-QCP. The same conclusion has been drawn on the basis of specific-heat and resistivity results on an "A"-type $CeCu_2Si_2$ polycrystal which has been tuned through $T_A \rightarrow 0$ via hydrostatic pressure [29].

It is straightforward to relate this QCP to the disappearance of phase A at the critical coupling constant $g_c$ (Fig. 5). However, upon further approaching the QCP by cooling the single crystal to below 0.2 K, $\rho(T)$ and $C(T)$ behave very disparately: While the resistivity (at sufficiently low fields) keeps varying as $\Delta\rho \propto T^{3/2}$ down to 20 mK, the lowest temperature of our experiment, the n-state specific-heat coefficient $\gamma(T)$ does <u>not</u> follow the corresponding $T^{1/2}$ dependence anymore (Fig. 6). Rather, it shows a steep upturn at low temperatures. Since this upturn cannot be ascribed to the Zeeman splitting of nuclear $^{63}Cu$, $^{65}Cu$ or $^{29}Si$ spin states through the external field (cf. solid lines in Fig. 6), an anomalous enhancement of the hyperfine coupling, i.e. an (average) finite "internal magnetic field" has to be invoked to account for this anomalous T dependence. The origin of this internal field is, however, not clear.

Upon increasing the magnetic field to $B > 6$ T one recognizes another surprising low-T property of our $CeCu_2Si_2$ single crystal. While the gross T dependence of $\gamma(T)$ remains unaffected (Fig.6), the $\Delta\rho(T)$ dependence becomes qualitatively changed into $\rho(T) = \rho_0 + aT^2$ (Fig. 7b). In addition, the $B = 14$ T data display the broadened transition into phase B which is not visible in $\gamma(T)$ measured at, e.g. $B = 12$ T (Fig. 6).

The $\rho(T) \propto T^2$ dependence suggests that phase B (as well as phase A, cf., e.g. Fig. 2 and [8]) forms out of a heavy Landau-Fermi-liquid phase - a notion which is, however, in conflict with the pronounced T dependences of $\gamma(T)$ precursive to both the B- and A-phase transition. The striking different T dependences of the resistivity for the $CeCu_2Si_2$ single crystal below and above $B \approx 6$ T are shown as $a(T) = \Delta\rho(T)/T^2$ vs T in Fig. 8a, along with the resistively determined B-T phase diagram in Fig 8b. We note that the field dependence of the limiting temperature $T_{lim}$ below which the $\Delta\rho = aT^2$ dependence is obeyed tracks that of the phase transition temperatures $T_B(B)$ and $T_A(B)$ for "A" and "AS"-type $CeCu_2Si_2$ [8]. From these observations one might be inclined to ascribe the $\Delta\rho = aT^2$ dependence preceding the A/B transitions to some critical fluctuations. However, assuming the A/B phases to be of itinerant nature, $\Delta\rho \propto T$ is predicted [30] in the critical regime $T > T_{A/B}$.

To summarize, n-state resistivity and specific-heat measurements performed in sufficiently low fields and at intermediate temperatures suggest the existence of a QCP of antiferromagnetic nature where $T_A \rightarrow 0$. This is concluded from the agreement of experimental data with theoretical predictions for a nearly antiferromagnetic Fermi liquid (NAFFL) in a one-band system of itinerant fermions [25-27]. However, upon approaching the QCP sufficiently closely, there are two striking observations that strongly violate this NAFFL scenario: 1) the absence of a crossover in $\Delta\rho(T)$ to a Landau-Fermi-liquid-type $T^2$ behavior (at least above 20mK). This suggests that singular scattering occurs on the <u>whole</u> Fermi surface rather than along some "hot lines" only. 2) $\Delta\rho(T)$ and $\gamma(T)$ behave very disparately. This indicates a breakdown of the concept of heavy quasiparticles. Rather it appears that, near the A-phase transition, their itinerant component (probed by $\Delta\rho(T)$) and the local 4f component (probed by $C(T)$) are decoupled from each other.

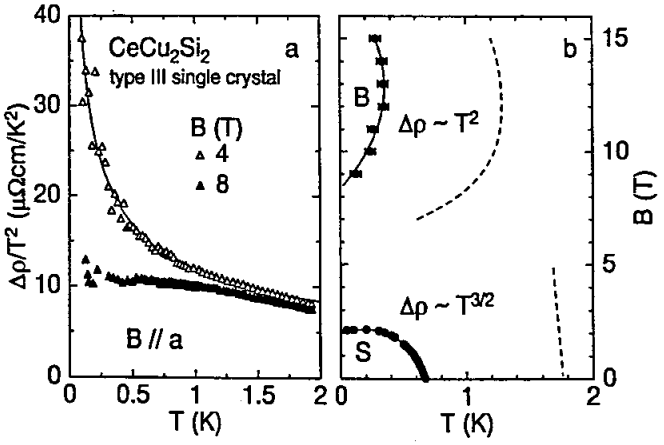


Fig.8. a: $\Delta\rho/T^2$ vs T ($\Delta\rho = \rho - \rho_0$) at B = 4 T and 8 T for the same "AS-type" $CeCu_2Si_2$ single crystal as in Figs. 6 and 7. Solid line marks $T^{-1/2}$ dependence of a(T) = $\Delta\rho(T)/T^2$.
b: B-T phase diagram for the same crystal derived from ρ(T) measurements. Existence ranges for superconductivity (S) and phase B are indicated along with limiting temperatures, $T_{lim}$, for $T^{3/2}$ and $T^2$ dependences of $\Delta\rho(T)$ (dashed lines).

## 3. $UBe_{13}$

Two variants of $UBe_{13}$ with markedly different sc- and n-state properties have been recently identified [31,32]: While "H-type $UBe_{13}$ exhibits $T_c$ values between 0.85 K and 0.9 K, "L-type" $UBe_{13}$ is characterized by $T_c \approx 0.75$ K. Most of the polycrystalline samples reported are of type H, while all L-type samples are single crystals.
In the following we discuss low-T properties of high-quality $UBe_{13}$ single crystals of the "H-type" variant.

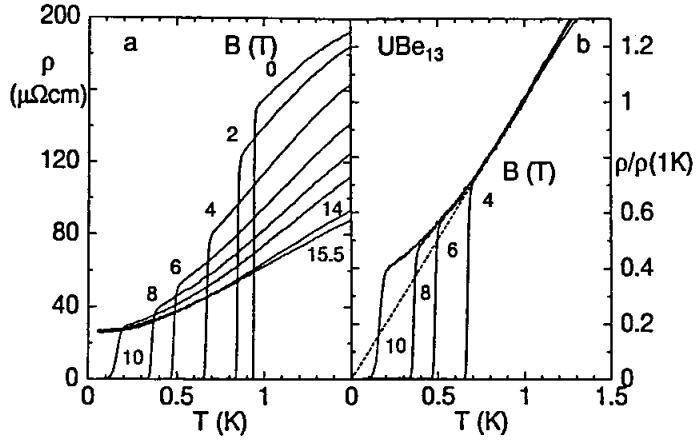


Fig. 9. a: ρ vs T for single crystalline $UBe_{13}$ at differing magnetic fields. b: Same data as in a, normalized to the respective ρ value at T = 1K. Dashed straight line is an extrapolation to T = 0 of the data for T ≥ 0.8K.

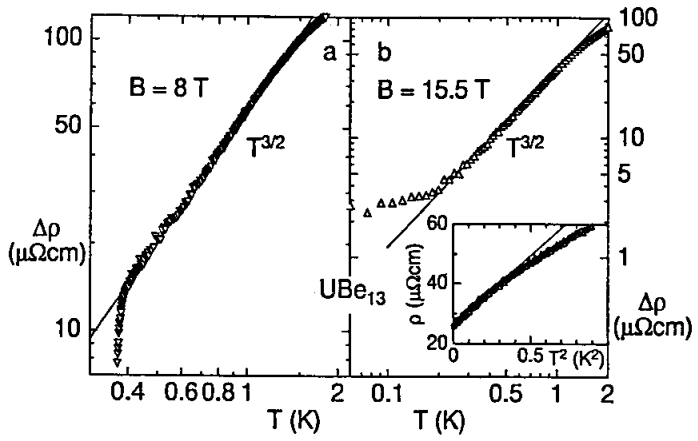


Fig. 10a,b. $\Delta\rho = \rho - \rho_0$ vs T (on logarithmic scales) for the same $UBe_{13}$ single crystal as in Fig. 9 at B = 8T (a) and B = 15.5T (b), respectively. Inset shows low-T data of (b) as $\rho$ vs $T^2$.

### 3.1 Non-Fermi-liquid normal state

Amongst HF compounds the superconductor $UBe_{13}$ [2] is one of the most prominent examples of a Non-Fermi-liquid-type normal state.

Besides a characteristic (Kondo) scale $T^*$ ranging from 8 K [33] to 30 K [34] which accounts for the large effective carrier masses another low-energy scale exists in this compound: At $T \approx 2K$ both thermodynamic properties, i.e. specific heat and thermal expansion as well as electrical resistvity [2] reveal more or less pronounced maxima (shoulders). From the maximum value of the resistivity, an inelastic mean free path as short as a few lattice spacings can be inferred. This anomaly has been commonly attributed to some, as yet unidentified, itinerant afm spin fluctuations [34]. On the other hand, as will be discussed below, the results of thermal-expansion measurements rather indicate these "2K fluctuations" to be of local (Kondo) type. As demonstrated in Fig. 9, already moderate fields are apt to suppress these fluctuation contributions efficiently: In a wide field range, $4\ T \le B \le 10\ T$, we are able to scale the various $\rho(T)$ curves within $T_c(B) < T \le 1.1K$ to a universal curve, by normalizing $\rho(T)$ by its respective value at T = 1K (Fig. 9b).

Above $T \approx 0.8$ K, a linear $\rho(T)$ dependence is found, that can be extrapolated to $\rho \approx 0$ for $T \to 0$. At lower temperatures the data follow a $\rho = \rho_0 + \beta T^{3/2}$ dependence. This is demonstrated in Fig. 10a for the B = 8 T data. Apparently, this NFL behavior is in full accord with the predictions for the 3D NAFFL [25-27]. A $T^{3/2}$ dependence is found even up to the highest fields applied, i.e. 15.5 T. However, the low-T data for $T \le 0.3$ K taken at high fields of B = 14 T and 15.5 T are better described by $\Delta\rho = \rho - \rho_0 = aT^2$, see inset Fig. 10b. The gigantic coefficient a is found to decrease with increasing field from 52 $\mu\Omega cmK^{-2}$ at B = 14 T to 45 $\mu\Omega cmK^{-2}$. We cannot decide whether this asymptotic $T^2$ term also exists at low fields, where it is masked by the sc transition, or whether it is induced by the high magnetic field. We note that already at low fields a crossover from a $T^{3/2}$ to $T^2$ at sufficiently low temperatures is required for a NAFFL [28]. Such a crossover, however, cannot be expected on the basis of isothermal n-state magnetoresistance results yielding $\Delta\rho(B) < 0$ below T = 2 K in the whole field range, B < 14 T. A negative sign of $\Delta\rho(B)$ is typical for NFL, while $\Delta\rho(B) > 0$ is a hallmark of the Landau FL. In fact, for $B \ge 14$ T $\Delta\rho(B)$ becomes positive at the same low temperatures where $\Delta\rho(T)$ follows the $T^2$ law.

To summarize, the NFL properties found for $UBe_{13}$ are consistent with the nearness of a QCP, though there is no clear-cut evidence for the presence of afm order at ambient pressure. A more detailed analysis of the NFL n-state properties is, however, hampered by the large value of its upper critical field. On the other hand, from the appearance of a positive peak in the thermoelectric power in pressurized (p > 23 Kbar) $UBe_{13}$ [35], a high-pressure AF ground state has been inferred which might be related to the present observations.

### 3.2 Revision of the phase diagram in $U_{1-x}Th_xBe_{13}$

First indications for the unconventional nature of the superconducting order parameter in $UBe_{13}$ stem from the observation of a $T^3$ dependence of the low-T specific heat [36]. Even more intriguing was the subsequent discovery of a non-monotonic $T_c(x)$ dependence for weakly Th doped $U_{1-x}Th_xBe_{13}$ [7], notably the occurrence of two subsequent phase transitions above a critical Th concentration $x_{cr} \approx 0.019 < x < 0.045$. So far, the origin of the lower of the subsequent transitions at $T_{c2} < T_{c1}$ is unclear. While early ultrasonic-attenuation measurements reveal indications for an AF transition [37], a superconducting nature of the transition has been claimed from measurements of the lower critical field [38]. In addition, the existence of very small magnetic moments of $\mu_s \approx 10^{-3}\mu_B/U$ for $T < T_{c2}$ has been deduced from muon-spin-relaxation ($\mu$SR) studies [39].
Attempting to explain the non-monotonic $T_c(x)$ dependence theoretical models started from the assumption of different anisotropic sc states for $x < x_{cr}$ and $x > x_{cr}$ as arising from the crossing of two different representations of the cubic symmetry group [40,41]. Studying various combinations of two respective representations Sigrist and Rice achieved a qualitative description of the above experimental results [41]. In their model, $T_{c2}$ marks the transition from a state belonging to a single representation for $T_{c2} < T < T_{c1}$ into a state formed by a combination of two representations. Since the latter is nonunitary it possesses magnetic

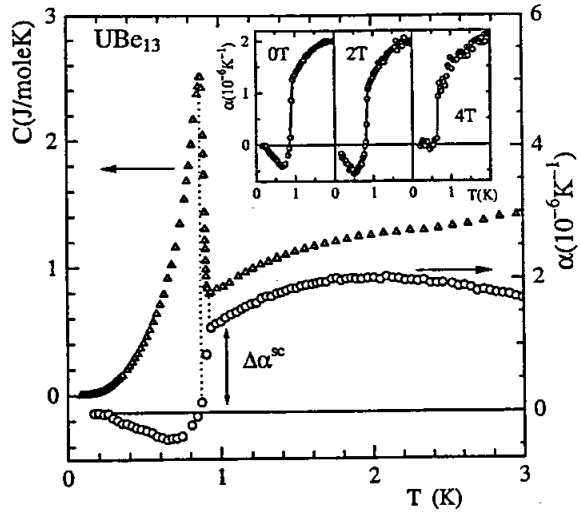


Fig. 11. Low-temperature specific heat (left scale) and thermal expansion (right scale) of single crystalline $UBe_{13}$ plotted on the same temperature scale. Width of superconducting transition is indicated by vertical dotted lines. Inset shows thermal expansion at varying fields.

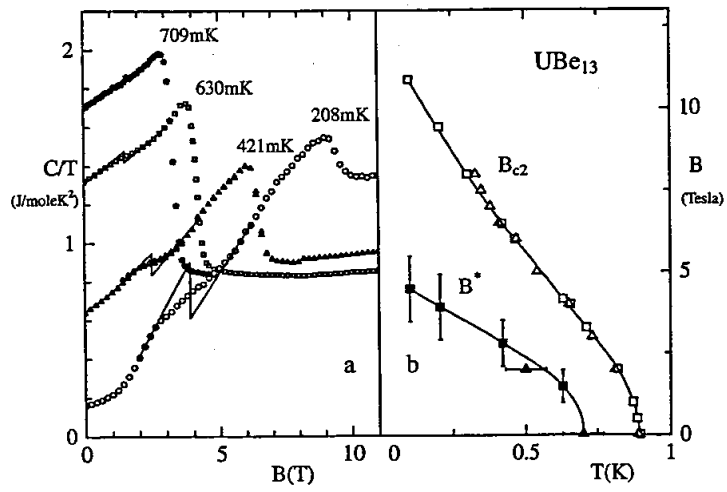


Fig. 12. a: Low-temperature specific heat as C/T vs B at varying temperatures of the same $UBe_{13}$ single crystal as in Fig. 11. b: Corresponding B-T phase diagram including the upper critical field, $B_{c2}(T)$, as determined by specific heat (open squares) and thermal expansion, (open triangles) as well as positions of anomalies observed as a function of temperature in $\alpha(T,B=const)$ (solid triangles) and magnetic field in $C(B,T=const)/T$ (solid squares) giving rise to a line of anomalies $B^*(T)$.

properties which then might account for the magnetic signatures found in the μSR experimens. In Fig. 11 we compare results of specific-heat and thermal-expansion measurements on the same high-quality $UBe_{13}$ single crystal by plotting the data sets on the same temperature scale. Compared to C(T), the $\alpha(T)$ data in the superconducting state display a rather non-monotonic T dependence suggesting the existence of a further anomaly below $T_c = 0.9$ K. In fact, by projecting the width of the sc transition from C(T) on the $\alpha(T)$ data (vertical lines in Fig.11) we find that the superconducting transition manifests itself in the steep decrease in $\alpha(T)$ at $T_c$ = 0.9K, thus leaving the broadened minimum as an independent anomaly. This assignment is corroborated by (i) a thermodynamic analysis of the sc transition and (ii) an investigation of the field dependence of $\alpha(T)$: (i) Employing the construction as indicated in Fig. 11 to extract the $\alpha(T)$ discontinuity at $T_c$, $\Delta\alpha^{sc}$, we are able to calculate the initial hydrostatic-pressure dependence of $T_c$ by means of the Ehrenfest relation, i.e. $(\partial T_c/\partial p)_{p\to 0} = T_c \cdot V_{mol} \cdot 3 \cdot \Delta\alpha^{sc}/\Delta C^{sc}$, where $V_{mol}$ = 81.3 $cm^3$/mole is the molar volume. The so-derived pressure coefficient of $(\partial T_c/\partial p)_{p\to 0}$ = -(13±4) mK/kbar is in perfect agreement with the $T_c$ shift observed under hydrostatic-pressure conditions of -(13±4) mK/kbar [42]. (ii) The $\alpha(T)$ minimum is almost completely suppressed by a field of 4 T which has, however, only little effect on the sc transition (inset Fig. 11). From these $\alpha(T)$ measurements at zero field, or at constant, finite fields as well as isothermal field scans of the specific heat (Fig. 12a) a "new line of anomalies", $B^*(T)$, has been established in the B-T phase diagram of $UBe_{13}$ (Fig. 12b).

In Fig. 13 we follow the evolution of the $\alpha(T)$ minimum as a function of increasing Th doping. Upon increasing x to 0.01, 0.017 and 0.0185 (Fig. 13a), being still subcritical, the minimum becomes grows and shifts to lower temperatures. Using the corresponding specific-heat results, we can separate from the $\alpha(T)$ data the sc jump anomaly, leaving behind the $\alpha(T)$ minimum. For lack of any other well founded criterion, the (steeper) high-T flank of this minimum is replaced by an "equal-areas construction" by an idealized sharp jump. This defines the positions of the anomaly $T_L(x)$ in Fig. 12. A comparison of the data for subcritical Th concentrations with

those for $x > x_{cr}$ (Fig. 13b) strongly suggests that the lower phase transition anomaly at $T_{c2}$ for $x > x_{cr}$ evolves out of the $\alpha(T)$ minimum in the subcritical concentration range: Being still similar to its outward appearance (i.e. sign and asymmetry) to that for $x < x_{cr}$, the minimum has become progressively deeper and sharper upon increasing x to 0.022 and 0.03, now revealing the character of a true phase transition. The respective transition temperatures as derived from an "equal-areas construction" in an $\alpha/T$ vs T plot are in good agreement with literature results, cf. Fig. 14.

The T-x phase diagram is supplemented by the "new line of anomalies" $T_L(x)$. As the central result of this study we propose that the anomaly at $T_L(x)$ (for $x < x_{cr}$) marks the precursor of the second phase transition at $T_{c2}(x)$ (for $x > x_{cr}$).

To interpret the broadened anomalies for $x < x_{cr}$ we have two possibilities: They manifest either an (inhomogeneously) broadened phase transition or some short-range ordering effects.

An anisotropic sc transition at the $T_L(x)$ - $T_{c2}(x)$ line is discarded for two reasons: (i) the sharpening of the anomaly upon increasing the impurity (Th) concentration, and (ii) the isotropic lattice response associated with the anomaly at $T_L(x)$ [10] both of which are in contrast to the expectation for a transition into a state with a gap anisotropy [40]. In particular, a combined-representation state below $T_{c2}$ as proposed in [41] must be ruled out, since this requires the crossing of two phase boundaries at $x_{cr}$.

Rather the broad shape as well as the negative sign of the $\alpha(T)$ anomaly at $T_L$ would be consistent with short range AF correlations. The sharpening of these features for Th concentrations in excess of $x_{cr}$ then indicates the onset of true long-range order.

Finally, we like to address the line denoted $T_{max}$ in the T-x phase diagram in Fig. 14. $T_{max}(0)$ denotes the position of the "2K anomaly" in the coefficient of thermal expansion. To follow its evolution as a function of Th doping we plot in Fig. 15 $\alpha(T)$ data for various x over a somewhat extended temperature range. Compared to resistivity and specific heat, this anomaly

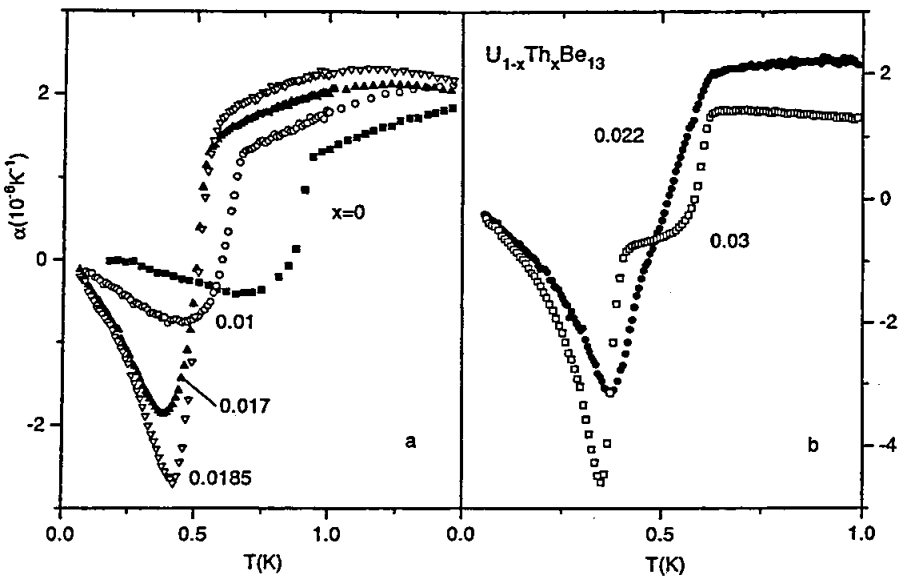


Fig. 13. Coefficient of thermal expansion of single crystalline $UBe_{13}$ and polycrystalline $U_{1-x}Th_xBe_{13}$ for x = 0.01, 0.017 and 0.0185 ($< x_{cr}$) (a) as well as x = 0.022 and 0.03 ($x > x_{cr}$) (b).

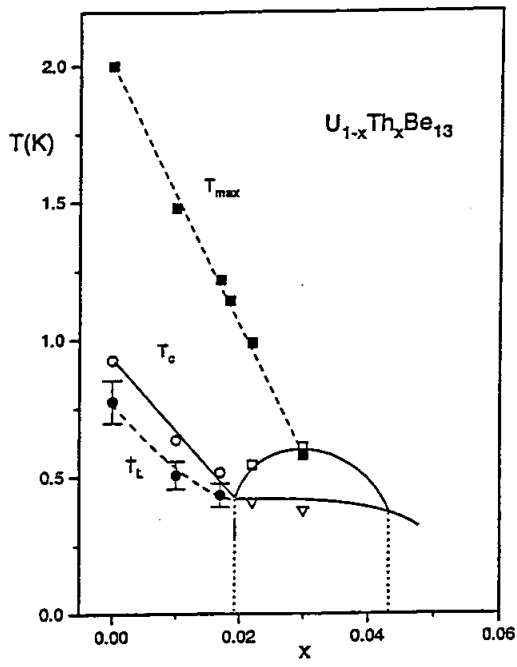


Fig. 14. T-x phase diagram of $U_{1-x}Th_xBe_{13}$ including results from literature [39] (solid lines) and the present study. Open symbols indicate second-order phase transitions, while closed symbols mark anomalies at $T_L$ and $T_{max}$ as described in the text. Vertical bars indicate uncertainties in determining $T_L$.

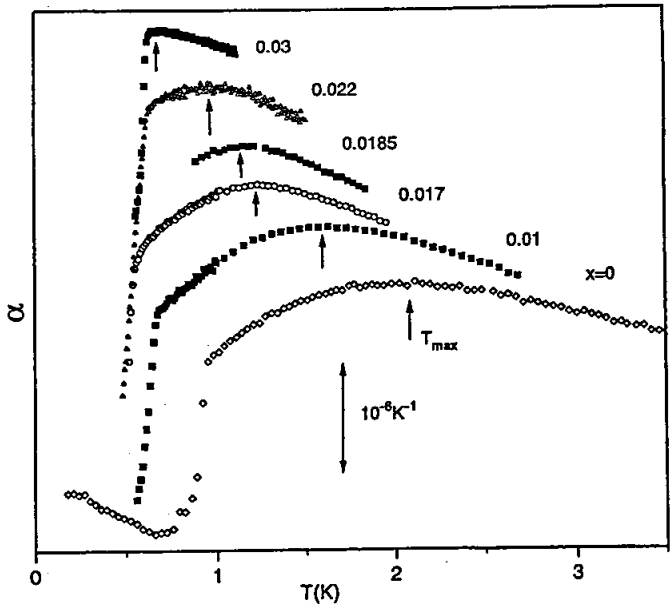


Fig. 15. Low-temperature thermal expansion of single crystalline $UBe_{13}$ and polycrystalline $U_{1-x}Th_xBe_{13}$. A vertical shift of each data set have been employed for clarity. Arrows mark the positions of the $\alpha(T)$ maximum.

is most strongly pronounced in $\alpha(T)$ which renders a background correction unnecessary. Most interestingly, and in contrast to the results of resistivity measurements [34], we find that $T_{max}(x)$ shows a linear reduction with x, hitting $T_{c1}$ at $x = 0.03$, i.e. right at its maximum value.
As already mentioned in Sect. 3.1 both the positive sign of $\alpha$ at the "2K anomaly" as well as the large corresponding Grüneisenparameter $\Gamma_{eff} \approx 50$ indicate the gradual freezing out of local Kondo-type spin fluctuations. This suggests an effective two-band scenario for $U_{1-x}Th_xBe_{13}$: HF superconductivity is carried by "less localized 5f states" with a characteristic temperature $T_{K1}$ = 8 - 30 K [33,34]. These states are scattered by Kondo fluctuations of the "more localized 5f states" with $T_{K2} \approx T_{max}(x)$. As long as $T_{max} > T_c$, these fluctuations are practically frozen out, i.e. harmless for superconductivity. Once $T_{max}$ becomes smaller than $T_{c1}$, however, an additional pair-breaking channel might open. This could be the case at $x = 0.03$ above which the pair-breaking character of these fluctuations causes $T_{c1}(x)$ to decrease, i.e. destabilizes the sc state.

To summarize, thermodynamic evidence is provided for a new line of anomalies in the T-x diagram of sc $U_{1-x}Th_xBe_{13}$. Although its nature cannot be established unambiguously by the present thermodynamic studies, our results rule out the models applied to this system so far and further constrain possible explanations for the various low-T phases of this canonical HF system.

## 4. Conclusions

The prototypical HF materials $CeCu_2Si_2$ and $UBe_{13}$ display significant NFL phenomena in their normal-conducting states. In either case our experimental findings indicate the existence of a "nearby" quantum critical point of antiferromagnetic type.
For $CeCu_2Si_2$, our investigations of different variants prove that the NFL normal state is neither necessary nor sufficient for the occurrence of HF superconductivity. Upon approaching the quantum critical point by further cooling the different response from resistivity on the one hand and specific heat on the other highlights a break-up of the itinerant and local (4f) parts of the heavy quasiparticles.
For $UBe_{13}$, our resistivity data indicate that the incoherent normal state is caused only to a smaller part by the so-called "2K-fluctuations". In addition, thermodynamic measurements provide evidence for a new line in T-x diagram of $U_{1-x}Th_xBe_{13}$ that marks the precursor of the lower transition at $T_{c2}$ for $x > 0.019$.

## Acknowledgements

We are grateful to W. Assmus for supplying the $CeCu_2Si_2$ single crystals. We gratefully acknowledge stimulating discussions with M. Sigrist and P. Thalmeier. Work in Darmstadt was supported by the BMBF grant NO. 13N6608/1. Work in Gainesville was supported by the DOE, Contract No. De-FG05-86ER45268.

## References

[1] F. Steglich, J. Aarts, C.D. Bredl, W. Lieke, D. Meschede, W. Franz and H. Schäfer, Phys. Rev. Lett. **43**, 1892 (1997).
[2] H.R. Ott, H. Rudigier, Z. Fisk and J.L. Smith, Phys. Rev. Lett. **50**, 1595 (1983).

[3] G.R. Stewart, Z. Fisk, J.O. Willis and J.L. Smith, Phys. Rev. Lett. **52**, 679 (1984).
[4] W. Schlabitz, J. Baumann, B. Pollit, U. Rauchschwalbe, H.M. Mayer, U. Ahlheim and C.D. Bredl, Abstr. ICVF5, Köln 1984 (unpublished); Z. Phys. B **62**, 171 (1986).
[5] C. Geibel, S.Thies. D. Kaczorowski, A. Mehner, A. Grauel, B. Seidel, U. Ahlheim, R. Helfrich, K. Petersen, C.D. Bredl and F. Steglich, Z. Phys. B **83**, 305 (1991).
[6] C. Geibel, C. Schank, S. Thies, H. Kitazawa, C.D. Bredl, A. Böhm, M. Rau, A. Grauel, R. Caspary, R. Helfrich, U. Ahlheim, G. Weber and F. Steglich, Z. Phys. B **84**, 1 (1985).
[7] H.R. Ott, H. Rudigier, Z. Fisk, J.L. Smith, Phys. Rev. B **31**, 1651 (1985).
[8] F. Steglich, P. Gegenwart, R. Helfrich, C. Langhammer, P. Hellmann, L. Donnevert, C. Geibel, M. Lang, G.Sparn, W. Assmus, G.R. Stewart, A. Ochiai, Z. Phys. B **103**, 235 (1997).
[9] P. Gegenwart, L. Donnevert, C. Langhammer, R. Horn, A. Link, C. Geibel, R. Helfrich, M. Lang, G. Sparn and F. Steglich (submitted).
[10] F. Kromer, R. Helfrich, M. Lang, F. Steglich, C. Langhammer, A. Bach, T. Michels, J.S. Kim and G.R. Stewart (submitted).
[11] M. Lang, R. Modler, U. Ahlheim, R. Helfrich, P.H.P. Reinders, F. Steglich, W. Assmus, W. Sun, G. Bruls, D. Weber and B. Lüthi, Physica Scripta T **39**, 135 (1991).
[12] G. Bruls, B. Wolf, D. Finsterbusch, P. Thalmeier, I. Kouroudis, W. Sun, W. Assmus, B. Lüthi, M. Lang, K. Gloos, F. Steglich and R. Modler, Phys. Rev. Lett. **72**, 1754 (1994).
[13] F. Steglich, P. Gegenwart, C. Geibel, R. Helfrich, P. Hellmann, M. Lang, A. Link, R. Modler, G. Sparn, N. Büttgen and A. Loidl, Physica B **223&224**, 1 (1995).
[14] Y. Uemura, W.J. Kossler, X.H. Yu, H.E. Schone, J.R. Kempton, C.E. Stronach, S. Barth, F.N. Gygax, B. Hitti, A. Schenck, C. baines, W.F. Lankford, Y. Onuki, T. Komatsubara, Phys. Rev. B **39**, 4726 (1989).
[15] H. Nakamura, Y. Kitaoka, H. Yamada, K. Asayama, J. Magn. Magn. Mat. **76&77**, 517 (1988).
[16] P. Thalmeier, Z. Phys. B **95**, 39 (1994).
[17] O. Trovarelli, M. Weiden, R. Müller-Reisener, M. Gómez-Berisso, P. Gegenwart, M. Deppe, C. Geibel, J.G. Sereni, F. Steglich, Phys. Rev. B **56**, 678 (1997).
[18] Y. Miyako, T. Takeuchi, T. Taniguchi, Y. Yamamoto, S. Kawarazaki, M. Acet, G. Dumpich, E.F. Wassermann, Z. Phys. B **101**, 339 (1996).
[19] R. Modler, Dissertation TH Darmstadt (1995) (unpublished).
[20] Kwak et al. Phys. Rev. Lett. **46**, 1296 (1981), D. Jérome, Science **252**, 1509 (1991).
[21] C. Geibel, Phys. Bl. **53**, 689 (1997).
[22] P. Gegenwart, M. Lang, A. Link, G. Sparn, C. Geibel, F. Steglich, W. Assmus, submitted to SCES '98, Paris, France.
[23] P. Gegenwart, Dissertation, TU Darmstadt (unpublished).
[24] R. Müller-Reisener, Diploma Thesis, TH Darmstadt (1995), unpublished.
[25] A.J. Millis, Phys. Rev. B **48**, 7183 (1993).
[26] G.G. Lonzarich, College on Quantum Phases, ICTP Trieste 1994, unpublished.
[27] T. Moriya and T. Takimoto, J. Phys. Soc. Jpn. **64**, 960 (1995).
[28] R. Hlubina and T.M. Rice, Phys. Rev. B **51**, 9253 (1995).
[29] F. Steglich, B. Buschinger, P. Gegenwart, M. Lohmann, R. Helfrich, C. Langhammer, P. Hellmann, L. Donnevert, S. Thomas, A. Link, C. Geibel, M. Lang, G. Sparn and W. Assmus, J. Phys.: Condens. Matter **8**, 9909 (1996).
[30] K. Ueda, J. Phys. Soc. Jpn. **43**, 1497 (1977).
[31] R. Helfrich, Dissertation, TU Darmstadt (1996), unpublished.

[32] C. Langhammer, R. Helfrich, A. Bach, F. Kromer, M. Lang, T. Michels, M. Deppe, F. Steglich, G.R. Stewart, J. Magn. Magn. Mat. **177-181**, 443 (1998).
[33] R. Felten, F. Steglich, G. Weber, H. Rietschel, F. Gompf, B. Renker, J. Beuers, Europhys. Lett. **2**, 323 (1986).
[34] E.A. Knetsch, Dissertation, University of Leiden (1993), unpublished.
[35] D. Jaccard, J. Sierro, J.P. Brison, and J. Flouquet, J. Physique **49**, C8-741 (1988).
[36] H.R. Ott, H. Rudigier, T.M. Rice, K. Ueda, Z. Fisk, J.L. Smith, Phys. Rev. Lett. **52**, 1915 (1984).
[37] B. Batlogg, D. Bishop, B. Golding, C.M. Varma, Z. Fisk, J.L. Smith, H.R. Ott, Phys. Rev. Lett. **55**, 1319 (1985).
[38] U. Rauchschwalbe, F. Steglich, G.R. Stewart, A.L.Giorgi, P. Fulde, K. Maki, Europhys. Lett. **3**, 751 (1987).
[39] R.H. Heffner, J.L. Smith, J.O. Willis, P. Birrer, C. Baines, F.N. Gygax, B. Hitti, E. Lippelt, H.R. Ott, A. Schenck, E.A. Knetsch, J.A. Mydosch, D.E. MacLaughlin, Phys. Rev. Lett. **65**, 2816 (1990).
[40] R. Joynt, T.M. Rice and K. Ueda, Phys. Rev. Lett. **56**, 1412 (1986).
[41] M. Sigrist and T.M. Rice, Phys. Rev. B **39**, 2200 (1989).
[42] S.E. Lambert, Y. Dalichaouch, M.B. Maple, J.L. Smith and Z. Fisk, Rev. Lett. **57**, 1619 (1986).

## DISCUSSION

**Sawatzky:** If I may make a comment. In RKKY theory the exchange interaction is usually described by delta function in real space and for rare earths the exchange is mostly due to 4f - 5d exchange interactions and the 5d character in the conduction electron sea is determined by the d-conduction electron hybridization. This mechanism uses the conduction electron states of local d symmetry. In the Kondo-like coupling derived from an Anderson like impurity Hamiltonian the exchange is derived starting from a hybridization of the f orbitals with the conduction electron states using therefore states of local f symmetry and then using a Schrieffer-Wolff transformation to get to the Kondo Hamiltonian. Note that these mechanisms use different symmetries of conduction electron states and are therefore not directly related. In addition one has the superexchanged terms I have mentioned before which destroy the simple relation between RKKY and Kondo-like terms.